

Realizing the Use of Molecular Electrocatalysts for Conversion of CO₂ to Multielectron Products

Arnab Ghatak* and Idan Hod*



Cite This: *Artif. Photosynth.* 2025, 1, 1–3



Read Online

ACCESS |

Metrics & More

Article Recommendations

The combustion of fossil fuels produces large amounts of carbon emission, thus posing a climate threat due to global warming.¹ Efforts on harnessing excess emitted CO₂ back to the carbon cycle via chemical, electrochemical, and photochemical pathways have seen steady development to produce value-added chemicals for energy storage.^{1,2} Among them, an environmentally benign electroreduction approach is the most promising one for valorization of CO₂ as fuels and chemicals, albeit the fact that sluggish kinetics and lack of selectivity require the design of suitable catalysts.^{3,4} Molecular electrocatalysts have well-defined active sites and accurately tailorable structures that allow mechanism-based performance optimization. Among them, several are based on easily available first-row transition metals to catalyze CO₂ reduction (CO₂RR) via a 2e[−]/2H⁺ mechanism to form CO and HCOOH.⁵ Nevertheless, examples of molecular catalysts capable of reducing CO₂ beyond 2e[−]/2H⁺ (e.g., multielectron products) are scarce. A key reason for that is the difficulty in controlling the binding affinity of the catalyst-bound CO intermediate, which often plays a pivotal role in the generation of multielectron/multiproton products.^{5,6} Along with this, the complexity of the multielectron/multiproton pathways involving multiple intermediates provides a limited understanding of the reaction mechanism.^{5,7} Herein, we would like to highlight several recently reported strategies that show promising CO₂RR activity and selectivity toward products beyond 2e[−]/2H⁺, such as (i) immobilization of functionalized molecular catalysts over conductive supports, (ii) incorporation of intramolecular hydrogen-bonding groups proximal to the active site, and (iii) the use of light illumination during electrochemical CO₂RR in molecular catalysts incorporated within porous hybrid platforms.

Initially, Wang et al. reported one of the first examples of a molecular electrocatalyst reducing CO₂ to value-added multi-electron hydrocarbons. They immobilized a cobalt phthalocyanine catalyst (CoPc, Figure 1a) over multiwalled carbon-nanotubes (CoPc/MWCNTs) and used it as a heterogeneous electrocatalyst that, in aqueous solution, undergoes 6e[−]/6H⁺ CO₂RR to generate CH₃OH.⁵ They first compared the catalytic performance of CNT-immobilized iron, cobalt, and nickel phthalocyanine (FePc, CoPc, and NiPc, respectively), as metal-to-CO binding energy, E_B(CO), varies with different M–N₄, spanning over a range of 1.2 eV and found that cobalt provides moderate CO binding. Therefore, among all three catalysts, only CoPc produced MeOH with a faradaic efficiency (FE) of up to 44% at −0.94 V vs RHE (CO and H₂ being the major products

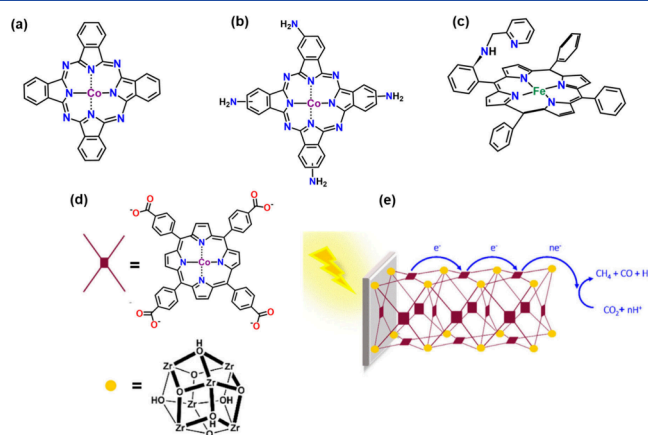


Figure 1. Catalysts (a) cobalt phthalocyanine and (b) cobalt phthalocyanine-NH₂ at the β position, used by Wang et al.⁵ (c) Catalyst FeL2, synthesized by Dey et al. with a second sphere pyridine moiety.² (d) Co-MOF-525 building units: CoTCPP linker and Zr₆(OH)₄O₄ node and (e) schematic representation of a photoassisted electrochemical CO₂ reduction reaction onto a FTO-Co-MOF-525 electrode by Hod et al.⁹ (d) and (e) are reproduced under a CC-BY 4.0 license from ref 9. Copyright 2023 Authors.

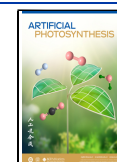
for FePc and NiPc). Through scanning transmission electron microscopy (STEM) analysis they have shown that CoPc has molecular level dispersion over the CNT, which is vital for MeOH formation. Otherwise, physical mixtures of CoPc and CNTs showed much less reactivity, despite having higher CoPc content. According to their observation, at lower overpotential, CO was the major CO₂RR product, and thus, it was postulated that CO acts as a reactive intermediate toward MeOH formation. Indeed, when an electrocatalytic CO reduction reaction (CORR) using CoPc/MWCNT was performed, it produced MeOH with a FE of 28% at −0.77 V vs RHE. Overall, catalysis goes through a “domino” process where CO₂ first reduces to CO, and then undergoes another 4e[−]/4H⁺ reduction to MeOH, and the potential-dependent steps of both CO₂RR

Received: July 7, 2024

Revised: August 1, 2024

Accepted: August 6, 2024

Published: August 30, 2024



and CORR are very similar. Nonetheless, this catalytic system suffers from rather limited durability. Upon only 1 h of electrolysis, $\text{FE}_{\text{CH}_3\text{OH}}$ decreased by 18%, while after 4 h of electrolysis, MeOH formation became negligible. UV–visible spectra of the postelectrolysis CoPc molecule from the electrode revealed an undesired reduction of the Pc ligand, eventually leading to hydrogenation of the macrocycle. To avoid the reductive deactivation, Wang and co-workers introduced four electron-donating amino groups in the β position of the CoPc moiety (Figure 1b, CoPc-NH₂), which successfully lowered the overpotential and could sustain activity for a longer time with a maximum $\text{FE}_{\text{CH}_3\text{OH}}$ of 32%.

At about the same time, Robert et al. also used the CoPc catalyst and MWCNT mixture with a Nafion binder over carbon paper for the conversion of CO₂ to MeOH.⁸ Under heterogeneous conditions in 0.5 M KHCO₃ solution (pH = 7.2), they obtained only 0.3% $\text{FE}_{\text{CH}_3\text{OH}}$ at −0.88 V vs RHE, which increased to 2% when they used CO as substrate instead of CO₂. However, at pH 13, when CO was used as a substrate, the same CoPc/MWCNT system exhibited 14.3% $\text{FE}_{\text{CH}_3\text{OH}}$ at −0.68 V vs RHE, i.e., a 50-fold increase in selectivity at a 170 mV lower overpotential, along with a 10-fold increase in catalytic rate. Subsequent HPLC experiments showed that during CORR at pH 13, formaldehyde (HCHO) is formed. At alkaline pH, there is a chance of Cannizzaro reaction, i.e., a disproportionation of HCHO (aldehyde without α hydrogens) to CH₃OH and HCOO[−] causing an overestimation of CH₃OH's FE determination. Knowing that, Robert and co-workers carefully evaluated these nonfaradaic CH₃OH formations and concluded that their effect is negligible. In addition, a series of control experiments, along with Co K-edge X-ray absorption near-edge structure (XANES) spectra of the CoPc before and after electrolysis proved that the observed reactivity was not due to the decomposition of CoPc into metallic Co nanoparticles, thus signifying the molecular nature of the catalyst.

Lately, McCrory et al. further investigated the catalytic properties of the CoPc/MWCNT system using a gas-diffusion electrode (GDE) flow-cell. Compared to a conventional H-cell configuration, performing the electrocatalytic reaction in a CO₂-fed GDE setup showed appreciably suppressed activity toward MeOH formation. The key explanation for these results lies at the higher CO₂ binding affinity of CoPc compared to its affinity to bind CO, as quantitatively measured in this study.⁶ The authors varied the partial current density of MeOH (product of CORR) at −0.70 V vs RHE as a function of the partial pressure of CO (P_{CO}), which ultimately reached a plateau at $P_{\text{CO}} = 1$. Thereafter, using a microkinetic analysis, the binding constant of CO to CoPc (K_{CO}) was determined to be 3.0 atm^{−1}. On the contrary, in the case of a CO₂RR reaction with CoPc (where the major product is CO), extracted K_{CO_2} was 11.1 atm^{−1}. The high binding constant ratio of $K_{\text{CO}_2}/K_{\text{CO}} = 3.7$, provides a thermodynamic explanation for the inefficient MeOH formation on CoPc/MWCNTs during CO₂RR, where catalyst-bound CO is preferentially displaced by CO₂ molecules before it can be further reduced. Thus, the authors suggested that researchers should look forward in the direction of controlling the local concentration of CO₂ by construction of catalyst–polymer composites, or via applying modifications to the coordination environments of CoPc. These strategies will strengthen the CO binding, especially when using GDE flow-cells.

As opposed to CoPc, in case of metal porphyrins, up until recently, reports of CO₂ reduction into multielectron compounds were only available when conducted under photochemical conditions.^{10,11} Lately, however, Dey and co-workers designed a distal superstructure in the molecular framework of iron porphyrins, and were able to stop the dissociation of CO from the metal-bound intermediate and simultaneously activated it for further reduction. In this work, an iron porphyrin having a distal basic pyridine residue was synthesized (FeL2, Figure 1c) and used as homogeneous electrocatalyst for CO reduction to CH₄, with 93% FE.² Spectro-electrochemistry coupled FTIR (FTIR-SEC) was employed to understand the mechanism of the reaction with in situ detection of the metal–carbonyl species, using ^{12/13}CO isotope sensitive absorption. In CO-saturated CH₃CN containing 3% H₂O, they identified an Fe^{II}–CO species being reduced to Fe^I–CO at applied potential of −1.75 V vs Fc/Fc⁺, followed by the reduction of Fe^I–CO to Fe⁰–CO at −2.35 V vs Fc/Fc⁺. Interestingly, while holding the potential at −2.35 V for a long period, an Fe^{II}–CHO adduct was detected, which then could be further reduced to CH₄. In this case, pyridine mediated hydrogen-bonding between water molecules (i.e., proton source) and Fe^I–CO intermediate allows its stabilization, and activation for further reduction to CH₄ (as evidenced by DFT calculation).

In another attempt to achieve multielectron CO₂ reduction using porphyrins, our group adopted a different approach, based on a photoassisted electrocatalysis pathway for multiproton/multielectron CO₂RR. To do so, we have utilized photoactive Co-porphyrin (CoTCPP)-based metal–organic framework (MOF) films (Co-MOF-525). Under 1-sun light illumination (100 mW/cm²), the MOF film can sustain large quantities of long-lived oxidized charged carriers during photocathodic operation and performed a 8e[−]/8H⁺ reduction of CO₂ to CH₄ (in 80/20 (%v/v) CH₃CN–H₂O with a LiClO₄ electrolyte).⁹ Subsequent, photoassisted chronoamperometric measurements revealed that in the potential window of −0.39 to −0.64 V, CH₄ and CO were produced during CO₂RR, with a maximum FE_{CH_4} being 14% at −0.49 V, while FE_{CO} was only 2%. Yet, in the absence of light illumination, both products were formed in a very negligible amount. At more cathodic potentials, a hydrogen evolution reaction (HER) became more prominent and significantly suppressed CO₂RR. Generally, Co^ITCPP is the CO₂RR active state that binds CO₂ and undergoes 2e[−]/2H⁺ reduction to CO. However, thin layer spectro-electrochemical measurements revealed a different mechanism that leads to the unexpected CH₄ production. Under dark electrolysis conditions, spectro-electrochemistry analysis showed the formation of bands attributed to Co^{II}TCPP and [Co^{III}TCPP]⁺, while measurements at more cathodic potentials showed the formation of a new band corresponding to CO₂RR active species, [Co^ITCPP][−]. Surprisingly, in photoassisted electrolysis conditions, the formation of a broad band at 460 nm was noticed, suggesting the existence of a higher oxidation form of the catalyst, namely, [Co^{III}TCPP]²⁺, which was the product of a porphyrin ring oxidation. Here, with an increase in the cathodic potential, the [Co^{III}TCPP]²⁺ band decreased in intensity, while the Co^{II}TCPP and [Co^{III}TCPP]⁺ bands remained unchanged throughout the course of the reaction. In other words, in these conditions, MOF-525 maintains a high concentration of [Co^{III}TCPP]⁺ species (via photo-oxidative accumulation of holes), which is known to stabilize CO by preferentially binding with it,¹² a crucial step that allows its further reduction to CH₄.

To conclude, despite severe challenges posed in the electrocatalytic conversion of CO₂ to multielectron products, successful reports of molecular catalysts capable of CO₂RR beyond 2e[−]/2H⁺ have increased lately. The results highlighted herein could help pave the way toward (i) rational catalyst design, (ii) improved structure–function correlation studies, and (iii) identification of key mechanistic factors necessary to understand molecular catalyst operation both in homogeneous as well as heterogeneous configurations. Nevertheless, realizing the next-generation of molecular catalytic systems will have to involve new approaches for the stabilization of key reactive intermediates while developing means for their assembly onto porous functional supports that allows the incorporation of secondary-sphere interactions to stir the CO₂RR path toward the desired products.

AUTHOR INFORMATION

Corresponding Authors

Idan Hod – Department of Chemistry and Ilse Katz Institute for Nanoscale Science and Technology, Ben-Gurion University of the Negev, Beer-Sheva 8410501, Israel; orcid.org/0000-0003-4837-8793; Email: hodi@bgu.ac.il

Arnab Ghatak – Department of Chemistry and Ilse Katz Institute for Nanoscale Science and Technology, Ben-Gurion University of the Negev, Beer-Sheva 8410501, Israel; orcid.org/0000-0003-3027-9359; Email: ghatak@post.bgu.ac.il

Complete contact information is available at:
<https://pubs.acs.org/10.1021/aps.4c00011>

Author Contributions

The manuscript was written through contribution of all the authors. All authors have given approval to the final version of the manuscript.

Notes

The authors declare no competing financial interest.

ACKNOWLEDGMENTS

This work is supported by the European Research Council (ERC) under the European Union's Horizon 2020 Research and Innovation Program with Grant Agreement No. 947665. This work was also partially supported by Israel Science Foundation (ISF; Grant No. 1267/22).

REFERENCES

- (1) She, X.; Wang, Y.; Xu, H.; Chi Edman Tsang, S.; Ping Lau, S. Challenges and Opportunities in Electrocatalytic CO₂ Reduction to Chemicals and Fuels. *Angew. Chem., Int. Ed.* **2022**, *61* (49), No. e202211396.
- (2) Patra, S.; Bhunia, S.; Ghosh, S.; Dey, A. Outer-Coordination-Sphere Interaction in a Molecular Iron Catalyst Allows Selective Methane Production from Carbon Monoxide. *ACS Catal.* **2024**, *14* (10), 7299–7307.
- (3) Cao, R. Across the Board: Rui Cao on Electrocatalytic CO₂ Reduction. *ChemSusChem* **2022**, *15* (21), No. e202201788.
- (4) Francke, R.; Schille, B.; Roemelt, M. Homogeneously Catalyzed Electroreduction of Carbon Dioxide—Methods, Mechanisms, and Catalysts. *Chem. Rev.* **2018**, *118* (9), 4631–4701.
- (5) Wu, Y.; Jiang, Z.; Lu, X.; Liang, Y.; Wang, H. Domino electroreduction of CO₂ to methanol on a molecular catalyst. *Nature* **2019**, *575* (7784), 639–642.
- (6) Yao, L.; Rivera-Cruz, K. E.; Zimmerman, P. M.; Singh, N.; McCrory, C. C. L. Electrochemical CO₂ Reduction to Methanol by Cobalt Phthalocyanine: Quantifying CO₂ and CO Binding Strengths

and Their Influence on Methanol Production. *ACS Catal.* **2024**, *14* (1), 366–372.

(7) Shen, J.; Kortlever, R.; Kas, R.; Birdja, Y. Y.; Diaz-Morales, O.; Kwon, Y.; Ledezma-Yanez, I.; Schouten, K. J. P.; Mul, G.; Koper, M. T. M. Electrocatalytic reduction of carbon dioxide to carbon monoxide and methane at an immobilized cobalt protoporphyrin. *Nat. Commun.* **2015**, *6* (1), 8177.

(8) Boutin, E.; Wang, M.; Lin, J. C.; Mesnage, M.; Mendoza, D.; Lassalle-Kaiser, B.; Hahn, C.; Jaramillo, T. F.; Robert, M. Aqueous Electrochemical Reduction of Carbon Dioxide and Carbon Monoxide into Methanol with Cobalt Phthalocyanine. *Angew. Chem., Int. Ed.* **2019**, *58* (45), 16172–16176.

(9) Ifraemov, R.; Mukhopadhyay, S.; Hod, I. Photo-Assisted Electrochemical CO₂ Reduction to CH₄ Using a Co-Porphyrin-Based Metal–Organic Framework. *Sol. RRL* **2023**, *7* (5), No. 2201068.

(10) Rao, H.; Lim, C. H.; Bonin, J.; Miyake, G. M.; Robert, M. Visible-Light-Driven Conversion of CO₂ to CH₄ with an Organic Sensitizer and an Iron Porphyrin Catalyst. *J. Am. Chem. Soc.* **2018**, *140* (51), 17830–17834.

(11) Rao, H.; Schmidt, L. C.; Bonin, J.; Robert, M. Visible-light-driven methane formation from CO₂ with a molecular iron catalyst. *Nature* **2017**, *548* (7665), 74–77.

(12) Mu, X. H.; Kadish, K. M. Oxidative electrochemistry of cobalt tetraphenylporphyrin under a CO atmosphere. Interaction between carbon monoxide and electrogenerated [(TPP) Co]⁺ in nonbonding media. *Inorg. Chem.* **1989**, *28* (19), 3743–3747.